ACS APPLIED MATERIALS & INTERFACES

Research Article

www.acsami.org

Different Hierarchical Nanostructured Carbons as Counter Electrodes for CdS Quantum Dot Solar Cells

Gouri Sankar Paul,[†] Jung Ho Kim, Min-Sik Kim, Kwangseok Do, Jaejung Ko, and Jong-Sung Yu*

Department of Advanced Materials Chemistry, Korea University, 208 Seochang, Jochiwon, ChungNam 339-700, Republic of Korea

Supporting Information

ABSTRACT: CdS quantum dot sensitized solar cells based on TiO_2 photoanode and nanostructured carbon as well as Pt as counter electrodes using iodide/triiodide and polysulfide electrolytes were fabricated to improve the efficiency and reduce the cost of solar cells. Compared with conventional Pt (η = 1.05%) and CMK-3 (η = 0.67%) counter electrodes, hollow core-mesoporous shell carbon (HCMSC) counter electrode using polysulfide electrolyte exhibits much larger incident photon to current conversion efficiency (IPCE = 27%), photocurrent density (J_{sc} = 4.31 mA.cm^{-2}) and power conversion efficiency (η = 1.08%), which is basically due to superb structural characters of HCMSC such as large specific surface area, high mesoporous volume, and 3D interconnected well-developed hierarchical porosity network, which facilitate fast mass transfer with less resistance and enable HCMSC to have highly enhanced catalytic activity toward the reduction of electrolyte shuttle.

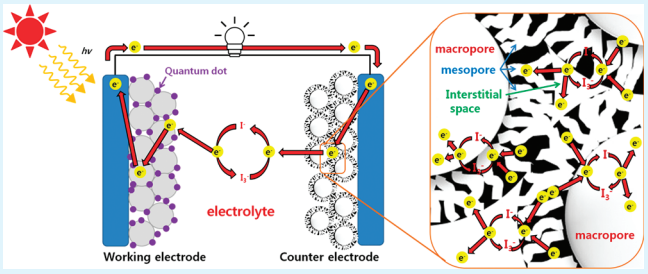

KEYWORDS: *mesoporous carbons, electrodes, CdS, quantum dots, solar cells*

INTRODUCTION

Quantum dot sensitized solar cells (QDSSCs) represent a key class of cell architecture that has emerged as a promising candidate for the development of next generation solar cells because of their acceptable power conversion efficiency and low production cost.[1,2] SSCs are based on the photosensitization of semiconductor photoanodes, typically nanocrystalline TiO_2, by absorbed dye or quantum dot sensitizers. The electron transport in a semiconductor medium is thus the key for device performance.

Recently, semiconductor nanocrystalline particles such as CdS,[3] CdSe,[4] and PbS[3,5] that absorb visible or near-infrared light have been used as alternate sensitizers in SSCs. Advantages of inorganic semiconductor sensitizers over conventional dyes are their high extinction coefficient and large intrinsic dipole moment that leads to rapid charge separation.[6] In particular, quantum dots (QDs), a special class of semiconductor nanoparticles exhibiting the quantum confinement effect, enable us to tailor the optical properties such as the band gap by controlling the particle size. In addition, it has been reported that the process of multiple exciton generation (MEG) can occur under specific excitation conditions of semiconductor nanoparticles.[7,8] However, the efficiency of QDSSC is still very low, and the reasons for this are not yet clearly understood. One of the possible reasons is the difficulty of assembling a sufficiently large number of QDs on a mesoporous TiO_2 matrix in order to obtain a well-covered monolayer without cluster formation or aggregation.[9] Other possible reasons include the higher charge recombination rate between QDs and electrolytes and also the presence of surface states possessing both electron and hole traps in the sensitizing semiconductors, which results in lower short circuit current and open-circuit photovoltage.[6,10] The retardation of charge recombination between sensitizers and electrolytes and blocking of the surface states were achieved through the surface passivation of sensitizers by using ZnS,[4,6] amorphous TiO_2 layer,[11] etc.

On the other hand, CdS may be directly grown on the surface of a wide band gap TiO_2 semiconductor (the electron-transport matrix) by means of different techniques. The most common processes include chemical bath deposition (CBD)[12,13] and spray pyrolysis.[14] The properties of the semiconductor material and the final performance of the solar cell will depend strongly on the preparation method, that is, colloidal CdS SSCs can present good performance but low QD loading, or alternatively, CBD confers high semiconductor loading to the SSCs but could lead to higher internal recombination in the closed-packed QD structure.[15] Recently, successive ionic layer adsorption and reaction (SILAR)[3,16] process was introduced to prepare CdS QDs and have drawn great attention during last couple of years. The preparation method also affects the charge-transfer kinetics.[17] Semiconductors directly grown on the electron-transport surface require thickness optimization for the wide band gap semiconductor film. Although thick layers increase the light absorption, they have other associated drawbacks such as

Received: October 21, 2011
Accepted: December 1, 2011
Published: December 1, 2011

reduced cell performance originating from the presence of sensitizer crystals directly grown on the electron-transport surface, leading to higher recombination.[18,19] Thick layers may also cause a reduced wetting of the semiconductor pores by the hole transporter, consequently decreasing the regeneration efficiency.[20] Basically, both the choice of preparation method and the type of semiconductor used influence the final performance of SSCs and need to be taken into account during the device optimization process. Apart from the efficiency, the cost-effectiveness of mass fabrication is equally important for a widespread of solar cell applications.

The counter electrode is also an important component of dye and quantum dot SSCs. FTO loaded with platinum and sputtered Au has been most frequently used as the counter electrode in SSCs. However, cost consideration necessitates the development of alternative material. In addition, there are also some reports on corrosion of Pt in triiodide-containing solutions.[21,22] Therefore, it is highly desirable to develop alternative cheap materials for the counter electrodes. Recently, different mesoporous and nanostructured carbons have been used as counter electrodes in DSSC.[23−27] Till date only few groups reported carbon counter electrode-based QDSSCs.[24,28] However, energy conversion efficiency (η) is still very low for the QDSSCs, ca. 3.90% for the CdSe quantum dots solar cell using mesoporous carbon as a counter electrode.[28] Therefore, further enhancement in η is necessary for practical application of QDSSCs.

In the literature, various redox couples including Co(II)/Co(III),[29−31] Fe^{2+}/Fe^{3+},[32] triethanolamines,[33,34] and mixed systems of redox couples[13] have been employed as substitutes of I^-/I_3^- to enhance the durability of DSSCs. However, these studies are mainly focused on DSSCs using dyes of ruthenium complexes. For QD-sensitized photoelectrodes using cadmium chalcogenide (S, Se, or Te) as sensitizers, a redox couple of polysulfide (S^{2-}/Sx^{2-})[35,36] may be a suitable system for stabilizing the QDs. Polysulfide redox couples were commonly prepared using aqueous solution and employed for photoelectrochemical cells with a three-electrode configuration. Only few papers were reported for the application in a practical solar cell that has a sandwich structure.[37,38] Diguna et al. used an aqueous polysulfide solution for a TiO_2 inverse opal electrode with pore sizes of 300−400 nm.[37] Tachibana et al. utilized a polysulfide electrolyte for a CdS-sensitized solar cell with nanocrystalline TiO_2 electrode and compared its performance with other redox systems.[38]

In this paper, we present the photovoltaic characteristics of CdS QDSSCs through the modification of counter electrode by using different mesoporous carbons like CMK-3 and hollow core-mesoporous shell carbon (HCMSC) as well as common Pt. HCMSC possesses superior structural characteristics such as large specific surface area, high mesoporous volume and particularly 3D interconnected unique hierarchical nanostructure consisting of hollow macropore core, mesoporous shell and interconnected large interstitial spaces between the packed spherical carbon particles. Here CdS QDs are prepared by SILAR process, and I^-/I_3^- or polysulfide is used as a charge mediator electrolyte. To the best of our knowledge, this represents the first SILAR process based CdS QDSSCs with nanostructured carbons as counter electrodes. A large improvement in efficiency to 1.05% is achieved using polysulfide electrolyte as compared to 0.48% in I^-/I_3^- electrolyte for the CdS QDSSC based on the pure TiO_2 photoanode and Pt counter electrode. In particular, the HCMSC counter electrode using polysulfide electrolyte has demonstrated considerably improved photovoltaic characteristics of CdS QDSSCs compared to CMK-3 and Pt counter electrodes.

EXPERIMENTAL SECTION

Commercially available glass substrate coated with F-doped SnO_2 (FTO) (Hartford glass; about 8 ohm/sq cm) was used as transparent conducting oxide (TCO) to prepare the TiO_2 photoelectrode and different counter electrodes (Pt, HCMSC and CMK-3). It was cleaned by successive immersion in acetone, deionized (DI) water, and ethanol in an ultrasonic cleaner before cell fabrication.

Preparation of Different Carbon Counter Electrodes. The HCMSCs (HCMSC-1 and HCMSC-2) were synthesized by replication through nanocasting of solid core/mesoporous shell (SCMS) silica, namely, the solid core and mesoporous shell of SCMS silica were transformed into the hollow core and mesoporous shell of HCMSC through the replication based on previous work.[39] To control the core size and shell thickness of HCMSC, the core size and shell thickness of SCMS silica were controlled through the addition of appropriate amounts of tetraethyl orthosilicate (i.e., 1 mL per gram of silica) and n-octadecyltrimethoxysilane (i.e., 0.5 mL) into the solution of solid silica spheres with proper size. Aluminum was also incorporated into the silica framework of SCMS silica through impregnation method to produce acidic sites on the surface of the silica.[39] A typical synthesis route for HCMSC is as follows. Phenol-paraformaldehyde was used as a carbon source to form phenol-resin/SCMS composite. Excess resin was removed by vacuum at ambient temperature. The resultant polymer/SCMS composite was heated under N_2 gas flow to 950 °C at a ramping rate of 3 K/min, and then carbonized at 950 °C for 7 h to produce carbon/SCMS composite. The silicate template was selectively dissolved by soaking the composite in a 2.0 M NaOH solution for 10 min followed by heating in an oven at 80 °C overnight. The template silica-free HCMS carbon product thus obtained was filtered, washed with ethanol and dried at 393 K overnight.

CMK-3, most representative ordered mesoporous carbon, was fabricated by replication through nanocasting of SBA-15 silica instead of SCMS silica using the same process.[40] Rod type SBA-15 silica ca. 850 nm in length and ca. 570 nm in diameter was synthesized according to the procedures reported elsewhere.[41] Aluminum was also incorporated into the silicate framework through the same impregnation method as in SCMS silica to produce acidic sites on the surface of SBA-15 silica. Detailed information about synthesis of CMK-3 can be seen in earlier work.[40]

The HCMSC and CMK-3 counter electrodes were fabricated as follows. First, 100 mg of HCMSC or CMK-3 was dispersed in 10 mL of ethanol with 2.5 mL of 5% concentrated nafion (as a binder) and ultrasonicated for 30 min followed by overnight magnetic stirring to prepare homogeneous carbon slurry. Then the carbon slurry was coated onto an FTO glass substrate with a carbon loading of approximately 120 μg cm^{-2} by using a doctor blade. Finally, the electrodes were heat treated in a muffle furnace open to air at 400 °C for 15 min in to evaporate the solvent and nafion binder. For comparison, Pt counter electrodes with an optimized Pt loading of approximately 50 μg cm^{-2} on FTO glass were prepared according to a previous method.[42]

Surface Characterization of Carbon Materials. The morphologies of the carbon materials (HCMSCs and CMK-3) were investigated by scanning electron microscopy (SEM) and transmission electron microscopy (TEM). SEM images were obtained using a Hitachi S-4700 microscope operated at an acceleration voltage of 10 kV, and TEM analysis was operated on EM 912 Omega at 120 kV. N_2 adsorption and desorption isotherms were measured at 77 K on a KICT SPA-3000 Gas Adsorption Analyzer after the carbon was degassed at 423 K to 20 μTorr for 12 h. The specific surface areas were determined from nitrogen adsorption using the Brunauer−Emmett−Teller (BET) equation. Total pore volume was determined from the amount of gas adsorbed at the relative pressure of 0.99. Micropore volumes of the porous carbons were calculated from the analysis of the

adsorption isotherms using the Horvath–Kawzoe method. Pore size distribution (PSD) was derived from the analysis of the adsorption branch using the Barrett–Joyner–Halenda (BJH) method.

Preparation of CdS QD Sensitized TiO_2 Layer. The TiO_2 anode was prepared as reported elsewhere.[28] Typically, first, TiO_2 film of 10 μm in thickness was fabricated on FTO glass plate by using a doctor blade casting anatase TiO_2 paste (Dyesol). Scattering layers were deposited by the doctor blade casting a paste containing 400 nm sized anatase particles (Dyesol, DSL 18NR-O) and sintered at 500 °C for 30 min. Then CdS deposition on the TiO_2 films was performed by SILAR technique.[43] The film was dipped in an ethanol solution containing 0.33 M $Cd(NO_3)_2$ for 30 s, rinsed with ethanol, and then dipped for another 30 s into a 0.5 M Na_2S methanol solution and rinsed again with methanol. The two-step dipping procedure is considered to be one cycle. This sequential coating was repeated for several cycles. It is known that the amount of the CdS QDs assembled on the photoanode increases with the number of SILAR cycles. Too thin or too thick CdS layer is not beneficial to the performance of QDSSCs, and thus appropriate SILAR cycles is very important.[44,45] In our experiments, the best performance of QDSSCs can be achieved for the photoanode assembled with CdS in about 12 SILAR cycles.

UV–vis absorption spectra of the CdS QD sensitized TiO_2 photoelectrodes were analyzed with a UV–vis spectrometer (Shimadsu UV 3101PC). The as-prepared QD-sensitized electrodes and the carbon counter electrodes were employed to construct two-electrode solar cells, which were separated by using a 50 μm thick hot-melt ionomer film (Surlyn). Water/methanol (3:7 by volume) solution was used as a cosolvent of polysulfide electrolyte.[13] The electrolyte solution was prepared by a homogeneous mixture of 0.5 M Na_2S, 2.0 M S, and 0.2 M KCl. The active area of the cell was 0.24 cm^2. Electrochemical impedance spectroscopy (EIS) measurements were conducted with an impedance analyzer (Parstat 2273, Princeton) at zero bias potential and 10 mV of amplitude over the frequency range of 0.1 Hz to 100 kHz at a constant temperature of 20 °C. A sandwich cell consisting of two identical electrodes (active area 0.24 cm^2), a spacer of 50 μm thick Surlyn film, and a polysulfide electrolyte was used in the EIS measurements. Photocurrent–voltage measurement was performed with a Keithley model 2440 Source Meter and a Newport solar simulator system (equipped with a 1 kW xenon arc lamp, Oriel) at one sun (AM1.5, 100 mW/cm^2). Incident photon to current conversion efficiency (IPCE) was measured as a function of wavelength from 300 to 800 nm using an Oriel 300 W xenon arc lamp and a lock-in amplifier M 70104 (Oriel) under monochromator illumination, which was calibrated with a monocrystalline silicon diode.

RESULTS AND DISCUSSION

Figure 1a shows the respective SEM and TEM images of the as-synthesized HCMSC-1. SEM image (Figure 1a(i)) reveals that HCMSC-1 is generated as an individual uniform spherical particle with particle size of 350 nm, whereas the TEM image (Figure 1a(ii)) shows that the HCMSC-1 has a hollow core of approximately 300 nm in diameter and shell thickness of around 25–30 nm. The nitrogen adsorption–desorption isotherms of the HCMSC-1 are also shown at the Figure 1a(iii), which are of type IV with a H2 hysteresis according to the IUPAC classification, corresponding to framework mesopores. The pore size is estimated from the PSD maximum as approximately 3.2 nm. The HCMSC-1 exhibits a large BET surface area of 1600 m^2/g and a total pore volume of 1.52 cm^3/g, mainly attributable to the presence of the mesopores in the framework (mesopore volume: 0.72 cm^3/g). Figure 1b(i) and Figure 1b(ii) show the respective SEM and TEM images of HCMSC-2, which indicate that HCMSC-2 is an identical twin of the HCMSC-1, but with different particle size of 250 nm consisting of hollow core of approximately 200 nm in diameter and shell thickness of around 20–25 nm. N_2 adsorption–desorption isotherms and the derived PSD shown at the Figure

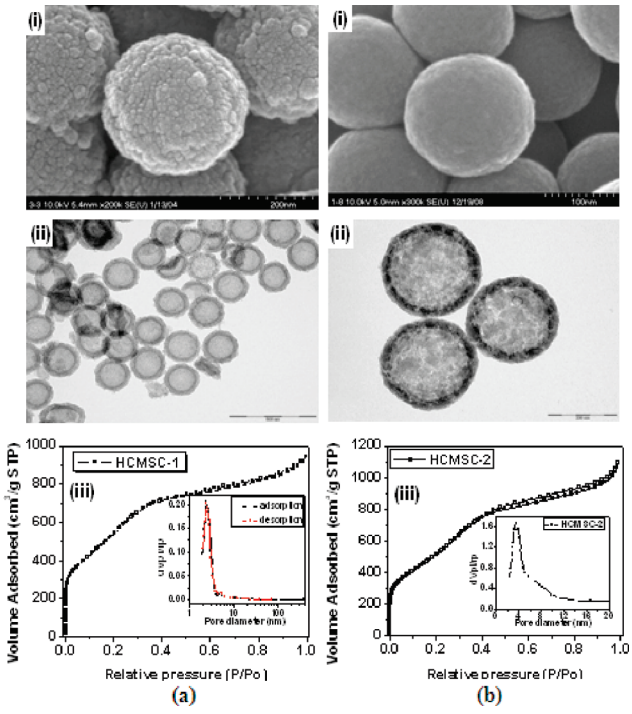

Figure 1. (i) SEM and (ii) TEM images and (iii) N_2 isotherms of (a) HCMSC-1 (300 nm core diameter and 25–30 nm shell thickness with average pore size obtained as 3.2 nm) and (b) HCMSC-2 (200 nm core diameter and 20–25 nm shell thickness with average pore size obtained as 3.4 nm).

1b(iii) reveal a BET surface area of 1950 m^2/g, a total pore volume of 1.72 cm^3/g, a mesoporous volume of 0.81 cm^3/g, and predominant mesopores centered at ca. 3.4 nm for the HCMSC-2.

Figure 2 shows the respective SEM and TEM images of CMK-3. SEM image (Figure 2(a)) reveals that CMK-3 is prepared as a uniform discrete short rod like structure with

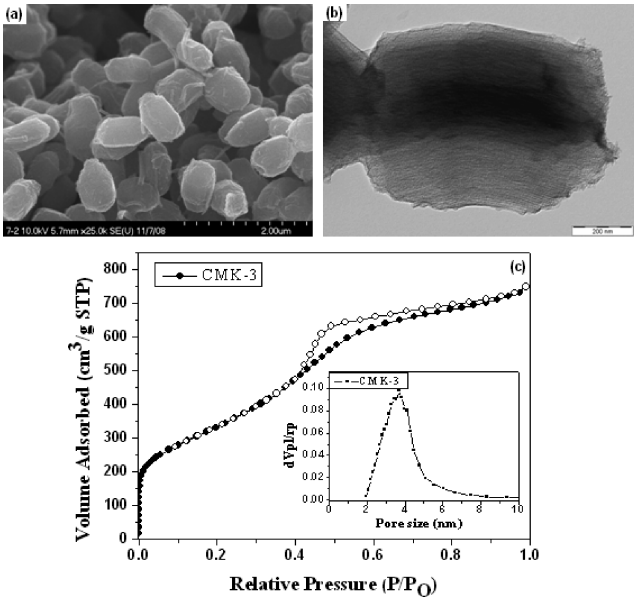

Figure 2. (a) SEM and (b) TEM images and (c) N_2 isotherms of CMK-3 with 570 nm in diameter and 850 nm in length with average pore size obtained as around 3.6 nm.

dx.doi.org/10.1021/am201452s | ACS Appl. Mater. Interfaces 2012, 4, 375–381

approximately 850 nm in length with diameter of approximately 570 nm, while TEM image (Figure 2(b)) shows well development of uniform mesopore channels running through the CMK-3 structure. N_2 adsorption−desorption isotherms and the derived PSD shown at the Figure 2(c) reveal a BET surface area of 1208.1 m^2/g, total pore volume of 1.15 cm^3/g, a mesoporous volume of 0.62 cm^3/g, and predominant mesopores centered at ca. 3.6 nm for the CMK-3. HCMSC possesses 3D interconnected unique hierarchical nanostructure (see Figure S1 in Supporting Information) consisting of hollow macropore core, mesoporous shell and interconnected large interstitial spaces between the packed spherical carbon particles, whereas CMK-3 reveals only a type of uniform mesopores in the framework. Table 1 summarizes the structural parameters based on N_2 adsorption−desorption isotherms of the studied

Table 1. Structural Parameters Based on N_2 Adsorption−Desorption Isotherms of the Studied Porous Carbon Materials

material	S_{BET} ($m^2\ g^{-1}$)	V_{total} ($cm^3\ g^{-1}$)	V_{meso} ($cm^3\ g^{-1}$)	pore size (nm)
HCMSC-1	1600.0	1.52	0.72	3.2
HCMSC-2	1950.0	1.72	0.81	3.4
CMK-3	1208.1	1.15	0.62	3.6

porous carbon materials, i.e., HCMSC and CMK-3 for a clear comparison in this work.

Schematic representation of the CdS QD sensitized TiO_2 photoanode is given in Scheme 1. In the present work, the CdS QDs are prepared by different SILAR processes (6, 9, 12, 15

Scheme 1. Typical Scheme of the CdS QD Preparation by SILAR Process[a]

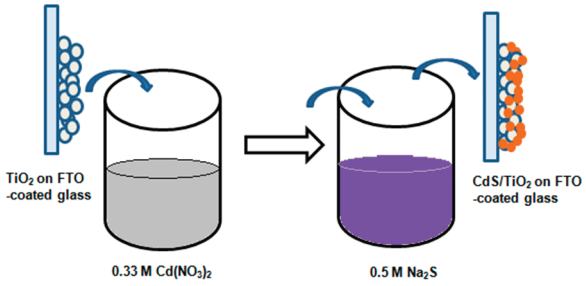

[a]The whole process is one cycle and repeated several times to increase the deposition of CdS QDs at TiO_2 on FTO-coated glass.

cycles etc.). As the SILAR cycle is increased, deposition of CdS QDs on the TiO_2 layer also increases and the films change from light yellow (for 6 cycles) to deep orange (for 15 cycles). SEM characterization has been performed on the CdS QD sensitized TiO_2 thin films deposited on FTO-coated glass substrates to observe the size and shape of the CdS QDs. The size of the spherical shape CdS QDs is measured around 20−30 nm (see Figure S2 in the Supporting Information). It is also observed that as the SILAR cycles are increased, thickness of the CdS layer increases, and the CdS QDs tend to agglomerate more with slightly increasing particle size. The CdS QDs deposited on FTO-TiO_2 substrates are highly adherent and yellowish orange in color. Optical properties of CdS films are measured by UV−Vis spectrophotometer in the wavelength range of 360−560 nm to evaluate the amount of the CdS incorporated in a TiO_2 film. The variation of the absorbance spectra is shown in Figure 3 for the films deposited with different SILAR cycles on the FTO-TiO_2 nanoporous films sintered at 500 °C. The

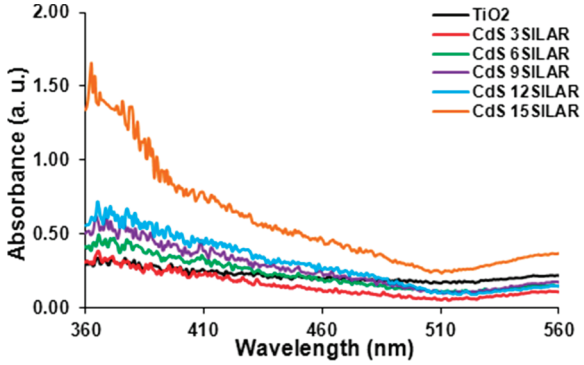

Figure 3. Absorbance spectra of the CdS QD-sensitized TiO_2 photoanodes, where CdS QDs are deposited by different SILAR cycles.

absorbance spectra increase with an increase of SILAR cycles, indicating an increased adsorption amount of CdS. Figure S3 represents the absorption spectra of the same samples in the extended wavelength range of 360−800 nm. A very broad signal is observed in the range of 510−700 nm for all the CdS QD sensitized TiO_2 photoanodes, which may be ascribed to some unknown background signal.

Figure 4a shows the current density vs voltage characteristics of the CdS QDSSCs prepared by different SILAR cycles with Pt counter electrode and I^-/I_3^- electrolyte. Efficiency of the CdS QDSSCs is increased with the increase of SILAR cycles, and maximum efficiency (0.48%) is obtained for 12 SILAR cycles, which is consistent with the earlier literature.[16] When the CdS deposition is further increased, efficiency decreases drastically (0.27% for 15 SILAR cycles), which is basically due to the increase in thickness of the CdS QD layer. As the thickness is increased, series resistance of the solar cells also increases which decreases the performance of the cells. Physical parameters like open circuit voltage (V_{oc}), current density (J_{sc}), fill factor (FF) and efficiency (η) of the CdS QDSSCs with Pt counter electrode and I^-/I_3^- electrolyte are summarized in Table 2.

It is well-known that I^-/I_3^- electrolyte is corrosive to semiconductor nanomaterials, which degrades the stability of the QDSSCs. To improve the stability as well as overall efficiency polysulfide electrolyte was also used in CdS QDSSCs, and different physical parameters were examined in Figure 4b. It is observed that when polysulfide electrolyte is used instead of I^-/I_3^-, fill factor is increased from 20.17 to 49.21% and efficiency from 0.48 to 1.05% (see Table 3). Lee et al. have reported the conversion efficiency of 0.88% for CdS QDSSCs using Pt counter electrode and cobalt complex as electrolyte where CdS QDs are also prepared by SILAR process.[3] Polysulfide is reported to have a superior property in terms of cell performance and stabilization for the CdS as shown in this work.[38]

Because aqueous electrolyte always has a higher surface tension, it is difficult for this electrolyte to penetrate into the mesoporous matrix of a TiO_2 film. Without intimate contact between photoelectrode and electrolyte, the cell performance is poor. To solve this problem, other polar solvent such as alcohol has been used to substitute water. However, the dissociation of

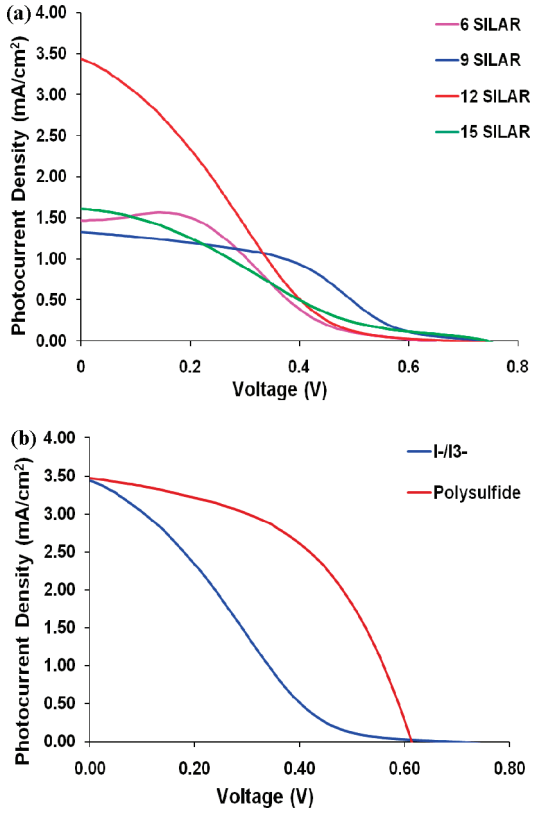

Figure 4. (a) $J-V$ characteristics of the CdS QD sensitized solar cells with Pt counter electrode using I^-/I_3^- electrolyte and (b) $J-V$ characteristics of the CdS QD (deposited by 12 SILAR cycles) sensitized solar cells with Pt counter electrode using two different electrolytes (I^-/I_3^- and polysulfide).

Table 2. Parameters of the CdS QDSSCs (Pt counter electrode and I^-/I_3^- electrolyte)

params	6 SILAR	9 SILAR	12 SILAR	15 SILAR
J_{sc} (mA/cm^2)	1.47	1.32	3.44	1.62
V_{oc} (V)	0.62	0.73	0.69	0.75
FF (%)	35.87	38.74	20.17	22.74
η (%)	0.33	0.37	0.48	0.27

Table 3. Parameters of the CdS QDSSCs (deposited by 12 SILAR cycles) with Pt Counter Electrode Using Two Different Electrolytes

	electrolytes	
params	I^-/I_3^-	polysulfide
J_{sc} (mA/cm^2)	3.44	3.47
V_{oc} (V)	0.69	0.61
FF (%)	20.17	49.21
η (%)	0.48	1.05

electrolyte in the alcohol is less than in the water. To consider both the penetration and ion dissociation abilities of the electrolyte, a cosolvent composed of alcohol/water is used for the polysulfide electrolyte. The optimal electrolyte solution was prepared by a homogeneous mixture of 0.5 M Na_2S, 2.0 M S, and 0.2 M KCl with 3:7 ratio of water/methanol as solvent.[13] Pt is a very efficient counter electrode for electrochemical solar cells which is also very expensive. To reduce the cost of the solar cells, different mesoporous carbons have been explored as counter electrodes to replace expensive Pt. Here we have used different nanostructured carbons (HCMSCs and CMK-3) as counter electrodes besides Pt. Figure 5a shows the current density vs voltage characteristics of CdS QD sensitized TiO_2

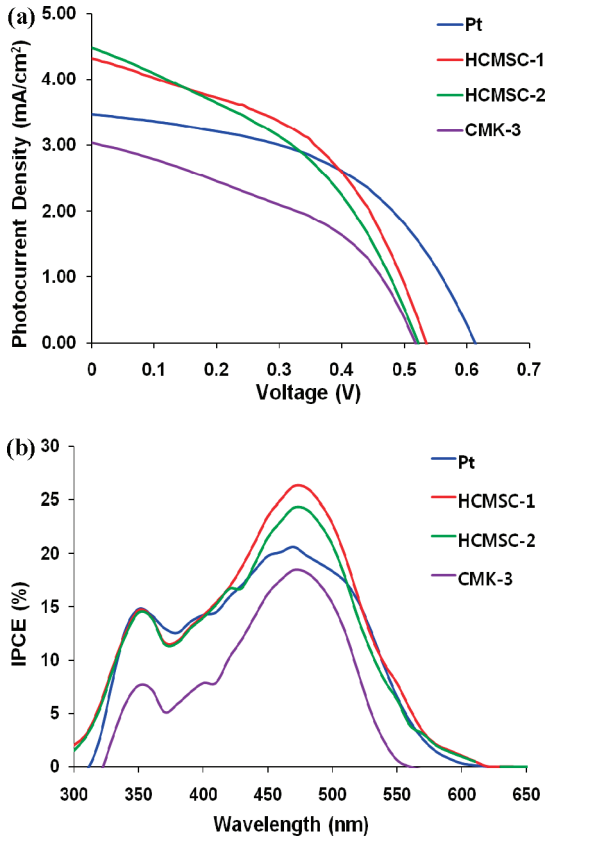

Figure 5. (a) $J-V$ characteristics and (b) IPCE curves of CdS QDSSCs prepared with different counter electrodes using polysulfide electrolyte.

based solar cells with different counter electrodes (Pt, HCMSCs and CMK-3) using polysulfide electrolyte. It is observed that 1.05% efficiency is obtained for Pt counter electrode whereas 1.08, 1.02, and 0.67% are obtained for HCMSC-1, HCMSC-2, and CMK-3, respectively, using polysulfide electrolyte (see Table 4). The efficiencies obtained for HCMSC counter electrode-based solar cells are comparable

Table 4. Parameters of CdS QDSSCs Prepared with Different Counter Electrodes Using Polysulfide Electrolyte

	counter electrodes			
params	Pt	HCMSC-1	HCMSC-2	CMK-3
J_{sc} (mA/cm^2)	3.47	4.31	4.50	3.04
V_{oc} (volt)	0.61	0.54	0.52	0.52
FF (%)	49.21	46.71	43.55	42.76
η (%)	1.05	1.08	1.02	0.67

to that of Pt counter electrode-based solar cell. So there is a lot of possibility to replace the Pt electrode by cost-effective novel nanostructured carbon such as HCMSC.

The IPCE is defined as the number of photogenerated charge carriers contributing to the current per incident photon. Figure 5b shows the IPCE curves of CdS QDSSCs prepared with different counter electrodes using polysulfide electrolyte.

dx.doi.org/10.1021/am201452s | ACS Appl. Mater. Interfaces 2012, 4, 375–381

The HCMSC-1 and HCMSC-2 counter electrode-based cells show maximum IPCE values of 27 and 24%, respectively, whereas for the Pt and CMK-3 based cells, the peak reaches to 21 and 18%, respectively, at 475 nm.

To find out the reasons for better performance of HCMSC counter electrode-based QDSSCs compared to other QDSSCs studied in this work, we carried out resistance measurements. To compare the resistances existing in the counter electrode and the electrolyte, we measured EIS spectra with the sandwich type electrochemical cells comprising two identical carbon (or Pt) counter electrodes. Figure 6a shows the equivalent circuit for this type of cell, where R_h is the ohmic serial resistance

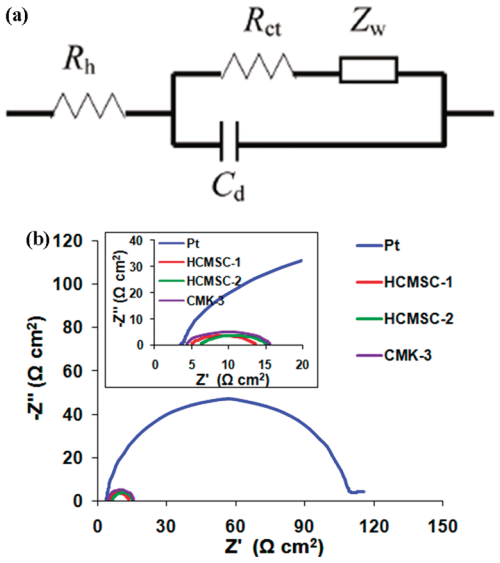

Figure 6. (a) Equivalent circuit of the electrochemical cell with identical electrode materials, and (b) Nyquist plots of Pt, HCMSCs, and CMK-3 counter electrodes in polysulfide electrolyte.

mainly related to the FTO glass, R_{ct} is the charge transfer resistance, C_d is the capacitance of electrical double layer, and Z_w is the Nernst diffusion impedance of the electrolyte. Figure 6b shows the typical Nyquist plots for the Pt, HCMSCs, and CMK-3 counter electrodes in polysulfide electrolyte, and the physical parameters determined for various counter electrodes are summarized in Table 5. It is found that the R_h values are at the same level for the various counter electrode materials while

Table 5. R_h, R_{ct}, and C_d Values of the Pt, HCMSCs and CMK-3 Counter Electrodes in Polysulfide Electrolyte

electrode	R_h (Ω cm^2)	R_{ct} (Ω cm^2)	C_d
Pt	3.76	49.86	0.15
HCMSC-1	4.36	6.47	3.67
HCMSC-2	5.08	7.02	3.27
CMK-3	3.94	8.25	3.05

a large difference was observed in the C_d values, namely, the carbon coated electrodes exhibit much larger (ca. 20 times) C_d values than that of the Pt electrode. Although the increased C_d values probably suggest larger electrochemically active areas for the carbon coated electrodes, it is still somewhat difficult for scientists to correlate quantitatively the C_d values with the electrochemically active areas. In contrast, the other parameter R_{ct} has been frequently used by scientists to evaluate the influence of the electrode materials on the performance of the solar cells. From Table 5, it is observed that Pt materials present high R_{ct} values (~50 Ω cm^2), implying much lower electrochemical catalytic activity in polysulfide electrolyte, which is consistent with the reported results.[28] Interestingly and importantly, the HCMSC electrodes present significantly decreased R_{ct}, ca. 6–7 Ω cm^2. Such low R_{ct} in the HCMSCs indicates that the HCMSC materials are very promising to improve the photovoltaic performance of the QDSSCs further. On the other hand, R_{ct} value of CMK-3 is ca. 8.25 Ω cm^2, which is slightly higher than the HCMSC, but lower than the Pt, also indicating the higher electrochemical catalytic activity than Pt in polysulfide electrolyte.

All the measurements were repeated several times to make sure that the values are constant. In such a system, an electrode material with high catalytic activity is highly desirable. As evident from the R_{ct} value, the HCMSC not only facilitates faster mass transport but also possesses higher catalytic activity toward the electrolyte. Enhanced catalytic activity is probably related to its superb hierarchical porous nanostructure of the HCMSC which is illustrated in Figure 7. The well-combined hierarchical structure with the mesopores in the shell open to

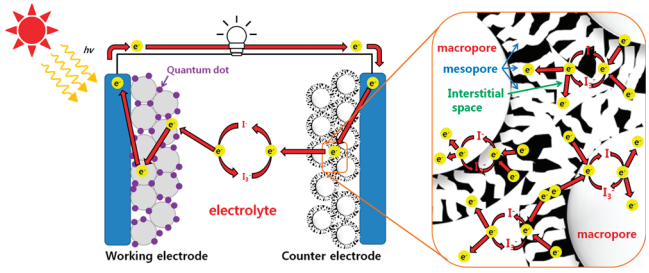

Figure 7. Schematic illustration of hierarchical porosity network around HCMSC counter electrode.

the outer surface and to the inner hollow macropore core provides an open highway network for efficient diffusion of reagents. Furthermore, the interconnected large interstitial spaces between the packed spherical carbon particles, unique in this system, are open to the mesoporous channels in the shell, providing other fast mass transport pathways. The enhancement in the mass transfer is expected to improve the photovoltaic performance in QDSSCs by increasing the fill factor (FF) of the solar cell and the short-circuit current density (J_{sc}).

CONCLUSIONS

CdS QDs are successfully deposited on TiO_2 electrode by different SILAR cycles. Fill factor as well as conversion efficiency of the CdS QDSSCs improved when polysulfide electrolyte is used instead of iodide/triiodide electrolyte. Efficiency obtained for polysulfide-based CdS QDSSC is 2 times higher than that of I^-/I_3^--based solar cell. The solar cell based on the HCMSC counter electrode using polysulfide electrolyte has demonstrated considerably improved IPCE (27%), photocurrent (4.31 mA cm^{-2}), and power conversion efficiency (1.08%) compared with solar cells base on Pt and representative ordered mesoporus carbon, CMK-3 counter electrodes, which likely result from the much lower R_{ct} value than that of the Pt, and the unique structural characteristics of the HCMSC such as a large specific surface area, high mesoporous volume, and 3D interconnected well-developed

hierarchical porosity network. The results presented in this study are very interesting and of particular significance not only because of the great improvement in the performance of solar cells but also because of the expected considerable decrease in the cost of fabricating solar cells. Thus, HCMSC counter electrode is considered suitable to replace the most expensive Pt counter electrode.

■ ASSOCIATED CONTENT

Supporting Information

A TEM/SEM image of HCMSC showing hierarchical porosity network (Figure S1); SEM images of the CdS QDs prepared by (a) 3 SILAR, (b) 6 SILAR, and (c) 12 SILAR process on TiO_2 layer deposited on FTO-coated glass substrate (Figure S2); UV−vis absorbance spectra of the CdS QD sensitized TiO_2 layer on FTO-coated glass substrates in the range of 360−800 nm (Figure S3). This material is available free of charge via the Internet at http://pubs.acs.org/.

■ AUTHOR INFORMATION

Corresponding Author

*E-mail: jsyu212@korea.ac.kr. Phone: +82-41-860-1494. Fax: +82-41-867-5396.

Present Address

†Electronic and Energy Materials Research Lab, Department of Materials Science and Engineering, Yonsei University, Seoul 120−749, Republic of Korea.

■ ACKNOWLEDGMENTS

This work was supported by a KRF grant funded by the Korea government (KRF 2010-0029245), the Ministry of Education, Science Technology through the Human Resource Training Project for Regional Innovation, and WCU (the Ministry of Education and Science) program (R31-2008-000-10035-0). The authors also thank the KBSI at Jeonju and Chuncheon for SEM and TEM analyses.

■ REFERENCES

(1) O'Regan, B.; Gratzel, M. *Nature* **1991**, *353*, 737.
(2) Lee, Y. L.; Lo, Y. S. *Adv. Funct. Mater.* **2009**, *19*, 604.
(3) Lee, H. J.; Yum, J. -H.; Leventis, H. C.; Zakeeruddin, S. M.; Haque, S. M.; Chen, P.; Seok, S. I.; Gratzel, M.; Nazeeruddin, M. K. *Langmuir* **2009**, *25*, 7602.
(4) Lee, Y. -L.; Huang, B. -M.; Chin, H. -T. *Chem. Mater.* **2008**, *20*, 6903.
(5) Hyun, B. -R.; Zhong, Y. -W.; Bartnik, A. C.; Sun, L; Abruna, H. D.; Wise, F. W.; Goodreau, J. D.; Matthews, J. R.; Leslie, T. M.; Borrelli, N. F. *ACS Nano* **2008**, *2*, 2206.
(6) Diguna, L. J.; Shen, Q.; Kobayashi, J.; Toyoda, T. *Appl. Phys. Lett.* **2007**, *91*, 023116.
(7) Beard, M. C.; Knutsen, K. P.; Yu, P.; Luther, J. M.; Song, Q.; Metzger, W. K.; Ellingson, R. J.; Nozik, A. J. *Nano Lett.* **2007**, *7*, 2506.
(8) Schaller, R.; Klimov, V. *Phys. Rev. Lett.* **2004**, *92*, 186601.
(9) Lee, H. Y.; Yum, J. -H.; Leventis, H. C.; Zakeeruddin, S. M.; Haque, S. A.; Chen, P.; Seok, S. I.; Gratzel, M.; Nazeeruddin, M. K. *J. Phys. Chem. C* **2008**, *112*, 11600.
(10) Hodes, G. *J. Phys. Chem. C* **2008**, *112*, 17778.
(11) Shalom, M.; Dor, S.; Ruhle, S.; Grinis, L.; Zaban, A. *J. Phys. Chem. C* **2009**, *113*, 3895.
(12) Chang, C.-H.; Lee, Y.-L. *Appl. Phys. Lett.* **2007**, *91*, 053503.
(13) Lee, Y.-L.; Chang, C.-H. *J. Power Sources* **2008**, *185*, 584.
(14) Hwang, J.-Y.; Lee, S.-A.; Lee, Y. H.; Seok, S.-I. *ACS Appl. Mater. Interfaces* **2010**, *2*, 1343.
(15) Mora-Sero, I.; Gimenez, S.; Fabregat-Santiago, F.; Gomez, R.; Shen, Q.; Toyoda, T.; Bisquert, J. *Acc. Chem. Res.* **2009**, *42*, 1848.
(16) Zhu, G.; Cheng, Z.; Lv, T.; Pan, L.; Zhao, Q.; Sun, Z. *Nanoscale* **2010**, *2*, 1229.
(17) Martínez-Ferrero, E.; Mora-Sero, I.; Alberoa, J.; Gimenez, S.; Bisquert, J.; Palomares, E. *Phys. Chem. Chem. Phys.* **2010**, *12*, 2819.
(18) Belaidi, A.; Dittrich, T.; Kieven, D.; Tornow, J.; Schwarzburg, K.; Lux-Steiner, M. *Phys. Status Solidi* **2008**, *2*, 172.
(19) Hodes, G. *J. Phys. Chem. C* **2008**, *112*, 17778.
(20) Gonzalez-Pedro, V.; Xu, X.; Mora-Sero, I.; Bisquert, J. *ACS Nano* **2010**, *4*, 5783.
(21) Kay, A.; Gratzel, M. *Sol. Energy Mater. Sol. Cells* **1996**, *44*, 99.
(22) Olsen, E.; Hagen, G.; Lindquist, S. E. *Sol. Energy Mater. Sol. Cells* **2000**, *63*, 267.
(23) Fang, B.; Fan, S.-Q.; Kim, J. H.; Kim, M.-S.; Kim, M.; Chaudhari, N. K.; Ko, J. J.; Yu, J. -S. *Langmuir* **2010**, *26*, 11238.
(24) Fan, S. -Q.; Fang, B.; Kim, J. H.; Jeong, B.; Kim, C.; Yu, J. -S.; Ko, J. J. *Langmuir* **2010**, *26*, 13644.
(25) Kyaw, A. K. K.; Tantang, H; Wu, T.; Ke, L.; Peh, C.; Huang, Z. H.; Zeng, X. T.; Demir, H. V.; Zhang, Q.; Sun, X. W. *Appl. Phys. Lett.* **2011**, *99*, 021107.
(26) Tantang, H.; Xiao, J.; Wei, J.; Chan-Park, M. B. E.; Li, L.-J.; Zhang, Q. *Eur. J. Inorg. Chem.* **2011**, *27*, 4182.
(27) Tantang, H.; Kyaw, A. K. K.; Zhao, Y.; Chan-Park, M. B. E.; Tok, A. I. Y.; Hu, Z.; Li, L. -J.; Sun, X. W.; Zhang, Q. *Chem. Asian J.* **2011**, DOI: 10.1002/asia.201100670.
(28) Fan, S.-Q.; Fang, B.; Kim, J. H.; Kim, J.-J.; Yu, J.-S.; Ko, J. J. *Appl. Phys. Lett.* **2010**, *96*, 063501.
(29) Sapp, S. A.; Elliott, C. M.; Contado, C.; Caramori, S.; Bignozzi, C. A. *J. Am. Chem. Soc.* **2002**, *124*, 11215.
(30) Cazzanti, S.; Caramori, S.; Argazzi, R.; Elliott, C. M.; Bignozzi, C. A. *J. Am. Chem. Soc.* **2006**, *128*, 9996.
(31) Yu, P.; Zhu, K.; Norman, A. G.; Ferrere, S.; Frank, A. J.; Nozik, A. J. *J. Phys. Chem. B* **2006**, *110*, 25451.
(32) Tian, Y.; Tatsuma, T. *J. Am. Chem. Soc.* **2005**, *127*, 7632.
(33) Nakanishi, T.; Ohtani, B.; Uosakin, K. *J. Electroanal. Chem.* **1998**, *455*, 229.
(34) Sheeney-Haj-Ichia, L.; Pogorelova, S.; Gofer, Y.; Willner, I. *Adv. Funct. Mater.* **2004**, *14*, 416.
(35) Vogel, R.; Hoyer, P.; Weller, H. *J. Phys. Chem.* **1994**, *98*, 3183.
(36) Licht, S. *Sol. Energy Mater. Sol. Cells* **1995**, *38*, 305.
(37) Diguna, L. J.; Shen, Q.; Kobayashi, J.; Toyoda, T. *Appl. Phys. Lett.* **2007**, *91*, 023116.
(38) Tachibana, Y.; Akiyama, H. Y.; Ohtsuka, Y.; Torimoto, T.; Kuwabata, S. *Chem. Lett.* **2007**, *36*, 88.
(39) Fang, B.; Kim, J. H.; Kim, M.-S.; Kim, M.; Yu, J.-S. *Phys. Chem. Chem. Phys.* **2009**, *11*, 1380.
(40) Yoon, S. B.; Kim, J. H.; Kooli, F.; Lee, C. W.; Yu, J.-S. *Chem. Commun.* **2003**, *14*, 1740.
(41) Kang, S.; Chae, Y. B.; Yu, J.-S. *J. Nanosci. Nanotechnol.* **2009**, *9*, 527.
(42) Kim, S. H.; Lee, J. K.; Kang, S. O.; Ko, J. J.; Yum, J. H.; Fantacci, S.; Angelis, F. D.; Censo, D. D.; Nazeeruddin, M. K.; Gratzel, M. *J. Am. Chem. Soc.* **2006**, *128*, 16701.
(43) Baker, D. R.; Kamat, P. V. *Adv. Funct. Mater.* **2009**, *19*, 805.
(44) Lee, H. J.; Leventis, H. C.; Moon, S. J.; Chen, P.; Ito, S.; Haque, S. A.; Torres, T.; Nuesch, F.; Geiger, T.; Zakeeruddin, S. M.; Gratzel, M.; Nazeeruddin, M. K. *Adv. Funct. Mater.* **2009**, *19*, 2735.
(45) Tak, Y. J.; Hong, S. J.; Lee, J. S.; Yong, K. J. *J. Mater. Chem.* **2009**, *19*, 5945.